REPORT DOCUMENTATION PAGE	Form Approved OMB No. 0704-0188

1. REPORT DATE (DD-MM-YYYY)	2. REPORT TYPE	3. DATES COVERED (From - To)
09-09-2005	PROCEEDING	

4. TITLE AND SUBTITLE	5a. CONTRACT NUMBER
QUANTIFICATION OF SEDIMENT PROPERTIES FROM PORE STRUCTURE AND GRAIN CONTACTS: A MICROCOMPUTED TOMOGRAPHY ANALYSIS OF SAX04 SANDS	5b. GRANT NUMBER
	5c. PROGRAM ELEMENT NUMBER N602782N

6. AUTHOR(S)	5d. PROJECT NUMBER
A.H. REED, K.E. THOMPSON, C.S. WILLSON, K.B. BRIGGS, M.D. RICHARDSON, AND B.T. HEFNER	5e. TASK NUMBER
	5f. WORK UNIT NUMBER

7. PERFORMING ORGANIZATION NAME(S) AND ADDRESS(ES)	8. PERFORMING ORGANIZATION REPORT NUMBER
Naval Research Laboratory Seafloor Sciences Branch Stennis Space Center, MS 39529	NRL/PP/7430-05-9

9. SPONSORING/MONITORING AGENCY NAME(S) AND ADDRESS(ES)	10. SPONSOR/MONITOR'S ACRONYM(S)
Office of Naval Research 800 North Quincy Street Arlington, VA 22217-5660	ONR
	11. SPONSOR/MONITOR'S REPORT NUMBER(S)

12. DISTRIBUTION/AVAILABILITY STATEMENT

Approved for public release; distribution is unlimited

13. SUPPLEMENTARY NOTES

Boundary Influences In High Frequency, Shallow Water Acoustics, Pages 83 - 90, University of Bath, UK 5th - 9th September 2005.

14. ABSTRACT

During the Sediment Acoustic eXperiment (SAX04), sediment physical properties (*e.g.*, porosity and permeability), determined by the arrangement of sand grains and the topology of the pore space, were evaluated in two ways: first, packing density in unconsolidated sand (d_{50} = 371 μm) was adjusted from minimum to maximum density by vibration; and second, diver-collected cores were impregnated with polyester casting resin to maintain pore and grain morphologies. Sediment pore-morphology and grain data was captured in volumetric x-ray Computed Tomography (CT) images (~10μm resolution) and quantified using a new grain-based algorithm. Porosity was calculated from the image data by voxel counting and permeability was determined using the Kozeny-Carman method, which is determined from porosity and grain size data. Grain contacts, an important determinant of frame modulus, were also determined. Bulk

15. SUBJECT TERMS

16. SECURITY CLASSIFICATION OF:			17. LIMITATION OF ABSTRACT	18. NUMBER OF PAGES	19a. NAME OF RESPONSIBLE PERSON
a. REPORT	b. ABSTRACT	c. THIS PAGE			Allen Reed
Unclassified	Unclassified	Unclassified	SAR	8	19b. TELEPHONE NUMBER (Include area code) 228-688-5473

QUANTIFICATION OF SEDIMENT PROPERTIES FROM PORE STRUCTURE AND GRAIN CONTACTS: A MICROCOMPUTED TOMOGRAPHY ANALYSIS OF SAX04 SANDS

A. H. REED

Marine Geosciences Division, Naval Research Laboratory, Stennis Space Center, MS 39576, USA
E-mail: allen.reed@nrlssc.navy.mil

K. E. THOMPSON

Dept. of Chemical Engineering, Louisiana State University, Baton Rouge, LA 70803, USA

C. S. WILLSON

Dept. of Civil and Environmental Engineering, Louisiana State University, Baton Rouge, LA 70803, USA

K. B. BRIGGS AND M. D. RICHARDSON

Marine Geosciences Division, Naval Research Laboratory, SSC, MS 39576, USA

B. T. HEFNER

Ocean Acoustics Dept., Applied Physics Laboratory, U. of Washington, Seattle, WA 98105, USA

During the Sediment Acoustic eXperiment (SAX04), sediment physical properties (*e.g.*, porosity and permeability), determined by the arrangement of sand grains and the topology of the pore space, were evaluated in two ways: first, packing density in unconsolidated sand (d_{50} = 371 μm) was adjusted from minimum to maximum density by vibration; and second, diver-collected cores were impregnated with polyester casting resin to maintain pore and grain morphologies. Sediment pore-morphology and grain data was captured in volumetric x-ray Computed Tomography (CT) images (~10μm resolution) and quantified using a new grain-based algorithm. Porosity was calculated from the image data by voxel counting and permeability was determined using the Kozeny-Carman method, which is determined from porosity and grain size data. Grain contacts, an important determinant of frame modulus, were also determined. Bulk porosity and permeability measurements from diver-collected cores (6-cm diameter) compared relatively well with image-based predictions. In general, sediment physical property values for laboratory packed sand were wider than those of the resin-impregnated and bulk samples. This study demonstrates the ability of high-resolution CT to image the micro-scale pore and grain morphology and of a new grain-based algorithm to quantify relevant features within these images. It is demonstrated that these features may then be used to quantify potential sediment physical properties for potential organizational states that may occur within a homogeneous sandy sediment that is reorganized by physical and biological forces.

A. H. REED ,K. E. THOMPSON, C. S. WILLSON, K. B. BRIGGS
. M. D. RICHARDSON , B. T. HEFNER

1 Introduction

1.1 *Select geoacoustic properties and relevant pore and grain scale parameters*

Sediment geoacoustic properties determine compressional wave speed and attenuation, and these properties change at varied spatial and temporal scales due to physical and biological forcing of wind waves, currents, and bioturbation that suspend, deposit, consolidate, and generally alter sediment morphology. Therefore, ranges of geoacoustic properties exist due to spatial and temporal variability in sediment packing that may correlate with the scales of the forcing. To determine the potential upper and lower bounds of geoacoustic properties (*e.g.*, porosity, permeability, and frame modulus) for the siliciclastic sediments that occur south of Ft. Walton Beach, FL, at the Sediment Acoustic eXperiment 2004 (SAX04) site, sediments were collected by divers and preserved. In this paper, we present data and properties extracted from a series of X-ray computed tomography (CT) scans of SAX04 sands, including resin-impregnated natural cores as well as cores packed to maximum and minimum density. A grain-based algorithm was used to quantify the properties of the sand grains as well as the pore geometry and topology. The physical properties of these systems can then be compared to results of results of field measurements of SAX04 geoacoustic properties and may also serve as potential upper and lower bounds for geoacoustic properties in SAX04 sands.

Pore-scale measurement of the pore and grain volumes enable calculation of porosity, the ratio of void space to total volume, and permeability, the area within the sediment that is available for fluid flow. CT images provide the high-resolution, three-dimensional datasets necessary for quantitative measurement of the void and pore space. Porosity is determined simply be dividing the number of void-space voxels by the total number of voxels in the system. Permeability may be determined using either modified Kozeny-Carman equations or Effective Medium Theory approaches [1,2]. For the permeability determinations, it has proved useful to determine the effective hydraulic radius of the pore space and to treat these pores as conduits for fluid flow. Permeability determined with the Kozeny-Carman equation, k_{ck}, is indirectly related, through grain size, to the interconnectedness of the pore space (*i.e.*, the pore coordination number), which has been shown to be important in both averaging (*e.g.*, Effective Medium Theory) and discrete methods (*i.e.*, Lattice-Boltzman simulations). However, the Kozeny-Carman equation is useful for determining permeability in well-rounded sands, where k_{ck} is determined as,

$$k_{ck} = \left[\frac{n^3 d_{50}^2}{180(1-n)^2} \right] \tag{1}$$

In equation 1, n is the fractional porosity and d_{50} is the mean grain diameter and the constant in the denominator accounts for the path length the a fluid must travel, which must vary as the sediment sample is compressed, repacked, or reorganized. Studies have shown that permeability and porosity may be the most important sediment properties affecting acoustic attenuation and sound speed dispersion [3]. However, concurrent with changes in these properties are changes in the sediment moduli. That is, the granular interactions that determine sediment compressibility become more or less rigid for different grain packings, depending upon the number and types of grain contacts. Evaluations of the grain packing by quantification of the grain contacts, may ultimately

enable determinations of frame modulus, currently a weakly understood phenomenon in naturally occurring sands that has proved difficult to evaluate with existing models [4]. The difficulty arises due to generalizations made by these models: sediments exist as a random packing of monosized spheres; porosity is non-varying; and grain contacts are "point-contacts" for which frictional influences are negligible (*i.e.*, no-slip conditions at contacts). A relationship between porosity and grain coordination number has been previously established; simply put grain coordination number (*i.e.*, the number of point contacts) increases as sample porosity decreases [5]. However, within these models, average grain coordination number is an important component that is rarely determined for natural sediments. For marine sand, porosities that range from 0.35 to 0.45 are reasonable estimates, and may be close to the lower and upper bounds of the SAX04 sands; for such porosities, according to Murphy [5], the grain coordination number could be expected to range from 9.5 to 7.3. Because, grain coordination number and porosity are important components of models that predict sediment moduli, this paper is addressing these parameters. Future work will be to quantify sediment moduli, and more importantly, make predictions of compressional and shear wave velocities from the mean grain coordination number, porosity and grain size.

In this paper, we quantify the solid and void phase properties of sands collected during SAX04, including resin-impregnated and reconstituted diver-core samples. It is also important to note that the aforementioned relationships between pore properties and acoustic properties are starting points from which compressional and shear wave velocities are determined, and that solutions to the Gassmann equation may be required to predict velocities in marine sand [6]. Although a rigorous analysis of predicted and measured velocities was not possible at this early date, our preliminary results indicate promise in using the approach presented in this paper for determining sound speed in natural sands, while still operating under an important Hertz-Mindlin assumption (*i.e.*, no-slip point contacts). In this case, the model would ignore frictional influences that determine sediment rigidity and operate at the face-to-face contacts (*i.e.*, contacts with large areal extent).

1.2   *Grain Based Reconstruction Algorithm – A tool for quantifying sediment components from high-resolution images*

The determination of the pore and grain properties starts with an evaluation of the spatial arrangement of pores and grains. This grain reconstruction algorithm transforms CT images of sediments into their more fundamental geological components (*i.e.*, grains, aggregates, pores) and has been useful in addressing complex grain shapes, such as quartz sand. This transformation is important because the form of the digital images (typically composed of tens of millions of voxels) is not amenable to direct physical analysis. Performing grain-scale reconstruction, however, allows computation of grain size distributions, pore and grain coordination numbers, surface areas, spatial correlations between pores, as well as other pore and grain parameters that are relevant to sediment physical and geoacoustic properties of natural sand.

We call this approach "grain-based" since the grain centers, located using a burn algorithm, serve as the basis for locating and defining the pore-grain structure in a three-step approach. The first step is to locate grain centers using a voxel burn of the solid

A. H. REED ,K. E. THOMPSON, C. S. WILLSON, K. B. BRIGGS
, M. D. RICHARDSON , B. T. HEFNER

phase. This is coupled with a nonlinear optimization process, if necessary. The second step is to merge grain centers in cases where the first step leads to repeated identification of the same grain (based on the maximum inscribed grain radius at each particle center). The third step is to perform a restricted voxel burn from the grain centers. This last step is a novel procedure that has proved successful for maintaining continuity in non-spherical grains and for ensuring proper division in cases where odd-shaped grains come into contact [2].

2   Methods

SAX04 sediments were carefully collected by scuba divers using hand-held, 6-cm diameter polycarbonate tubes and then carefully returned to the R/V Seward Johnson. Some of these cores were impregnated with polyester casting resin while the core was under vacuum while aboard ship. The solidified system was then subsampled by cutting the cores at 2-cm intervals with a rock saw and coring 8-mm-diameter samples from the center of the 2-cm-thick disks. Additional core samples were retrieved from the SAX04 site and sectioned into 2-cm intervals. These sections were evaluated for bulk density with conventional gravimetric methods and the grain size distribution was determined from the dried sections. A representative sample (standard splitting technique was used) was selected from the dried section, saturated with water, packed to near minimum imaged using high-resolution-CT scanning, repacked to near maximum density by vibration, and then imaged with the CT again. Diver cores were also collected for determination of permeability, which was determined on the ship using a constant-head permeameter.

The 8-mm-diameter resin-impregnated subsamples and the unconsolidated grain packings were x-rayed at high-resolution (~10 µm) using an x-ray Computed Tomography (CT) system that is housed at the Naval Research Laboratory. The industrial CT system operates in a range of 10-225 keV and 0-3 mA to produce images with maximum resolutions of <10 micrometers [7]. To achieve high-resolution images, or maximum magnification, samples were placed in close proximity to the focal spot opening of the X-ray tube and X-ray attenuation data were collected at a high number of line scans numerous times (*i.e.*, 2400 lines per 360° sample rotation with 6 integrations per line to yield well resolved and clearly differentiated pores and grains). The attenuation data were converted to image data using a back-filter algorithm and images were corrected for "beam-hardening", an artifact that occurs in images made from polychromatic energy sources. The images were then resampled, using a nearest-neighbor algorithm, to produce cubic voxels of ~10 µm in each of three dimensions. The 16-bit gray scale images were converted to 1-bit binary images (i.e., each voxel was designated as either solid or void) using an indicator kriging method in 3DMA [8]. A 300^3 subset of the image was then extracted for analysis using the grain-based algorithm. Three hundred voxels corresponds to ~8.5 grain diameters, based upon the mean grain size; this should provide a statistically representative sample.

3   Results of grain- and pore-scale evaluations

3.1   Pore and grain parameters for predictions of physical properties

Resin-impregnated sediment cores were chosen from the "Dalpod" (dc11_res) and "Rail" (dc19_res) sites; samples for the maximum and minimum density packings were taken from dried sections of non-impregnated cores, dc1 and dc24, corresponding to these two sites, respectively. The minimum and maximum values of gravimetrically determined sediment porosity in the 0-2-cm sand sections of diver cores were 0.354 and, 0.387 respectively [9]. Porosity values, based on the CT images of the resin-impregnated samples (Table 1), fall within this range. While the porosity values for the maximum and minimum packing of dc24 sand bound the resin-impregnated porosity (dc19_res), the porosity of maximum density packing of dc1 sand is greater than that for the resin-impregnated sample (*i.e.*, dc11_res). Two possibilities exist: 1) the packing of the resin-impregnated core is greater that that of the maximum density sample, or 2) segmentation errors occurred (*i.e.*, assigning individual voxels to either solid or void phases). Segmentation is one of the most difficult steps towards quantifying CT images.

Table 1. Values of pore and grain properties for the 0-2 cm depth interval from two SAX04 diver cores, dc11 and dc19, and maximum- and minimum-packed samples from sectioned cores dc1 and dc24. Dimensions are micrometers. nd = not determined

	dc11 res	dc1 max	dc1 min	dc19 res	dc24 max	dc24 min
Porosity	0.358	0.395	0.459	0.370	0.352	0.458
Permeability ($\times 10^{-11}$ m^2)	8.51	12.9	25.3	9.76	8.06	25.4
Inscribed Grain Radii	98.12	92.18	94.24	104.3	118.9	113.8
Grain Coordination #	7.72	6.88	5.60	6.63	8.04	5.92
Pore Radii	49.73	52.42	62.82	56.48	56.00	71.17
Pore Coordination #	5.71	6.52	6.85	5.95	5.75	6.53
Pore Throat Radii	35.00	35.99	41.86	38.79	38.97	48.04
Pore Throat Length	213.2	222.4	256.5	253.1	244.4	294.3
Ave Pore/Throat Aspect Ratio	0.651	0.640	0.611	0.627	0.648	0.614

A. H. REED ,K. E. THOMPSON, C. S. WILLSON, K. B. BRIGGS
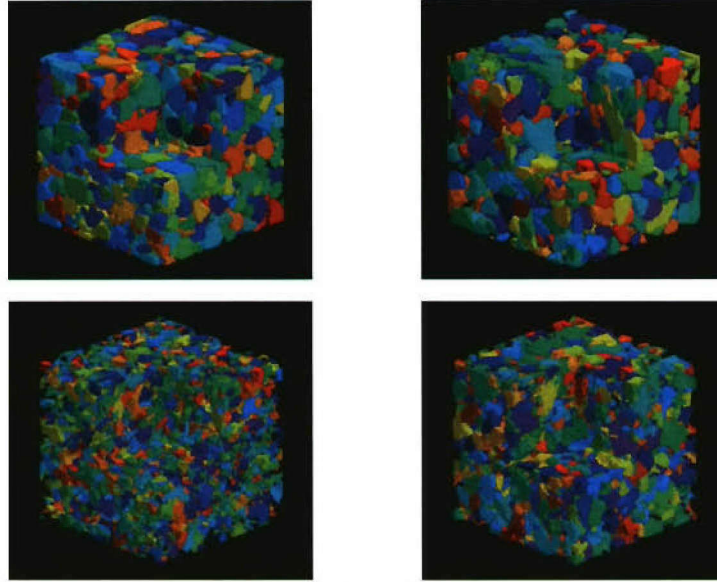, M. D. RICHARDSON , B. T. HEFNER

Figure 1. Maximum (left) and minimum (right) density packings of SAX04
sediments collected from the "Rail" site (dc24). Grains (top) and pores (bottom) are
false color coded to enhance visualization.

The minimum and maximum values of sediment permeability, determined from a constant-head permeameter test on 13-cm long cores, were 8.8×10^{-12} and 43.4×10^{-12} m^2, respectively. The average k_{ck} permeability value (calculated from equation 1) for these samples was 16.0×10^{-11} m^2, roughly ten times higher than constant-head values.

The grain-based algorithm was used to evaluate individual grains and pores (see Figure 1) and determine relevant properties (see Table 1). The CT imagery in Fig. 1 is presented in terms of grains (upper images) and pores (lower images), as well as maximum density packing (left) and minimum density packing (right). The pores in the maximum density packing appear smaller than the pores that occur in the minimum density packing, as would be expected. This qualitative result is confirmed; average pore radii in the maximum density samples are 15-20% smaller than in the minimum density samples (Table 1). Note that systems at maximum density packing have smaller throat radii and shorter throat lengths. Throat radii and length are fundamental properties related to permeability. It appears that the pore coordination number for the maximum density sample is less than for the minimum density sample while the pore/throat aspect ratio is larger. Additionally, these properties have a significant impact on multiphase flow (*e.g.*, drainage/imbibition, gas bubble migration).

Comparisons of the grain sizes between cores are determined as the effective grain size, which is the average of the inscribed grain diameter and the maximum grain length. Cumulative distributions of effective grain sizes are shown in Figure 2. For this data, grain size distributions for the maximum and minimum packing systems are very similar and the difference in the average grain radii is only a few percent (Table 1). Average

grain radii and particle size distributions for both resin-impregnated cores exhibit some differences compared to the maximum and minimum packing cores. It appears that the dc_11_res grain size distribution is similar to the dc_1 cores, yet grain sizes in dc_19_res are smaller and the distribution is broader than the dc_24 sands.

Particularly important in the calculation of sediment moduli are grain coordination numbers, which were determined with the grain-based algorithm and found to increase with increasing density. One of the primary advantages of the grain-based algorithm is the ability to uniquely identify each individual grain and it's properties.
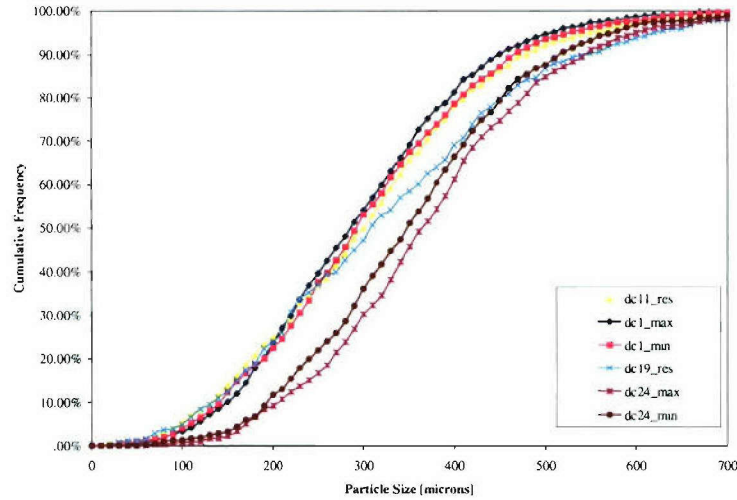

Figure 2. Frequency percent of effective grain size for select SAX04 sediment samples. "Dalpod" samples include dc11_res and dc1 and "Rail" samples include dc19_res and dc24.

4 Discussion

A grain-based algorithm is used to quantify high-resolution CT images of siliciclastic (quartz) sands collected from the SAX04 site and enables a several physical properties to be predicted for a range of packings. Values from CT-based imagery are relatively similar for porosity measurements and slightly higher for permeability than measurements presented by Briggs et al. [9]. Permeability values from the Kozeny-Carman formulation are reasonable for "clean" siliciclastic sands found in surficial marine deposits, however they are not in agreement with direct measurements. This may indicate that the simple approach taken, that is the prediction made by a derived formula of Kozeny-Carman, does not account for all the relevant parameters needed to accurately predict permeability in angular sediments. This is also made evident by the small effect that a fairly substantial change in pore throat properties had in this determination. Conceivably, as sediment was converted from minimum and maximum density packings (especially in dc24), a larger difference in permeability might occur, because pore throat sizes decrease markedly and the path length that a fluid travels through the sediment should simultaneously increase. This incongruity in the data will require further

evaluation or the utilization of more rigorous determination of permeability, which will enable the rejection of permeability predictions made using the Kozeny-Carman relationship, which may be better suited for less angular particles than exist at the SAX04 site. While the grain coordination numbers increase as sediment density increases, grain coordination values do not reach the assumed value, 9, commonly used for marine sediments. The relationship between coordination number and density may be addressed as the grain-based algorithm is further developed.

Future work will use more rigorous methods to estimate permeability (EMT, lattice-gas or Lattice-Boltzman) to incorporate pore size variability and pore coordination numbers. Relationships between the grain coordination, sediment moduli and sound speed in angular sediments will be evaluated using the Walton model [10].

Acknowledgements

References

1. Berryman, J. G. and Blair, S. C., Kozeny-Carman relations and image processing methods for estimating Darcy's constant. *J. Applied Phys.* **62**, 2221-2228 (1987).
2. Reed A. H., Briggs, K. B. and Lavoie D. L., Porometric properties of siliciclastic marine sand: a comparison of traditional laboratory measurements with image analysis and effective medium modeling. *IEEE J. Oceanic Eng.* **27(3)**, 581-592 (2002).
3. Williams, K. L, Jackson, D. R., Thorsos, E. I., Tang, D. J. and Schock, S. G., Comparison of sound speed and attenuation measured in a sandy sediment to predictions based upon Biot theory or porous media. *IEEE J. Oceanic Eng.* **27(3)**, 417-428 (2002).
4. Mavko, G., Mukerji, T. and Dvorkin, J., *The Rock Physics Handbook: tools for seismic analysis on porous media,* (Cambridge University Press, 1998), 329 pp.
5. Murphy, W. F., III, *Effects of Microstructure and Pore Fluids on the Acoustic Properties of Granular Sediment Materials*, Ph. D. dissertation, Stanford University (1982).
6. Bachrach, R., Dvorkin, J. and Nur, A., High-resolution shallow-seismic experiments in sand. Part II: velocities in shallow unconsolidated sand. *Geophysics* **60**,1234-1240 (1998).
7. Reed, A. H., *Computed Tomography at the Naval Research Lab*, (NRL web page, 2004), http://www7430.nrlssc.navy.mil/facilities/CTScanner/index.htm
8. Oh, W. and Lindquist, W. B., Image thresholding by indicator kriging. *IEEE Trans. Pattern Anal. Mach. Intell.* **21**, 590-602 (1999).
9. Briggs, K. B., Zimmer, M. and Richardson, M. D., Spatial and temporal variations in sediment compressional wave speed and attenuation measured at 400 kHz for SAX04. *Proc. Inst. Acoust.*, this volume (2005).
10. Walton, K., The effective elastic moduli of a random packing of spheres, *J. Mech. Phys. Solids* **35**, 213-226 (1987).